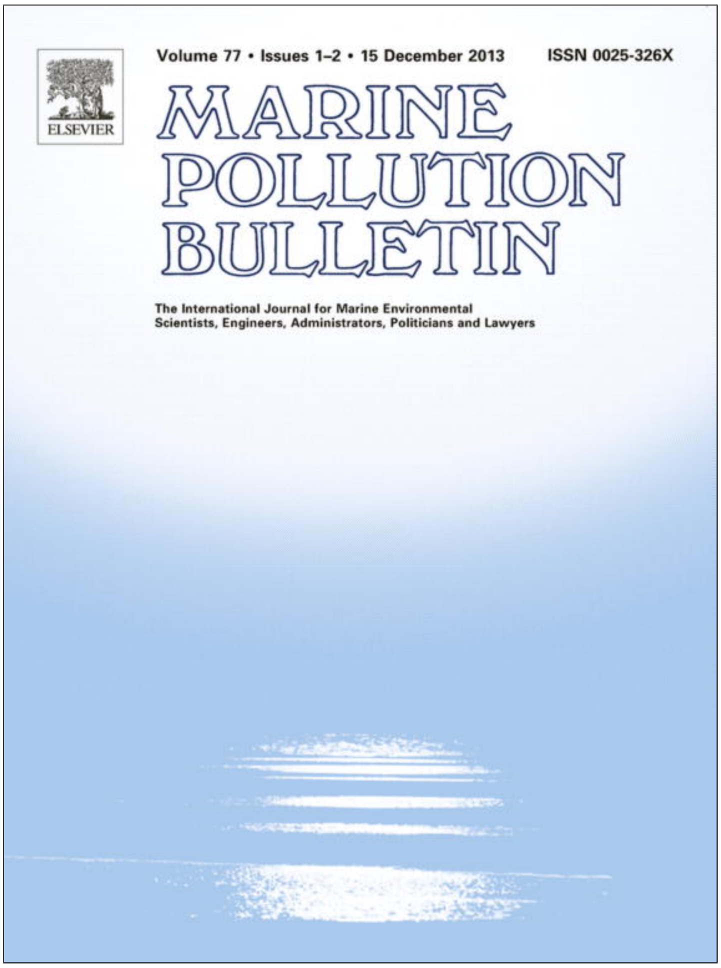
Volume 77 • Issues 1–2 • 15 December 2013
ISSN 0025-326X
ELSEVIER
MARINE POLLUTION BULLETIN
The International Journal for Marine Environmental
Scientists, Engineers, Administrators, Politicians and Lawyers

Marine Pollution Bulletin 77 (2013) 266–273

Contents lists available at ScienceDirect

Marine Pollution Bulletin

journal homepage: www.elsevier.com/locate/marpolbul

Analysis of a beach as a time-invariant linear input/output system of marine litter

Tomoya Kataoka [a,b], Hirofumi Hinata [a,*], Shigeru Kato [b]

[a] Coastal Zone Systems Division, Coastal, Marine and Disaster Prevention Department, National Institute for Land and Infrastructure Management, 3-1-1 Nagase, Yokosuka, Kanagawa 239-0826, Japan

[b] Department of Architecture and Civil Engineering, Toyohashi University of Technology, 1-1 Hibarigaoka, Tempaku, Toyohashi, Aichi 441-8580, Japan

ARTICLE INFO

Keywords:
Nii-jima Island
Linear system analysis
Unit impulse response
Residence time
Diffusion equation
Mark-recapture experiment

ABSTRACT

The exponential decay of the amount of new litter on Wadahama Beach, Nii-jima Island, Japan revealed by 20-month mark-recapture experiments demonstrates a linear response of the beach to the input of target items. Here we show the amplitude and phase characteristics of the beach as a time-invariant linear input/output system and discuss the hydrodynamic and geomorphological factors that would determine the characteristics with the aid of a diffusion equation. The characteristics are fully determined by the residence time of the items (τ_r = 209 days) and can be described as functions of the ratio of τ_r to the period of input variability. The decay is reproduced well by the analytical solution of the equation with a constant diffusion coefficient (D), whose order was estimated by τ_r and the backshore width. Generally, D would depend on hydrodynamical statistics and beach geomorphology as well as the dimensions and density of the items.

1. Introduction

The exponential decay of the amount of new litter on Wadahama Beach, Nii-jima Island, Japan revealed by 20-month mark-recapture (MR) experiments demonstrates a linear response of the beach to the input of litter. Here we show the amplitude and phase characteristics of the beach as a time-invariant linear input/output system and discuss hydrodynamic and geomorphological factors which would determine the system characteristics by analyzing a diffusion equation.

A number of beach surveys on the abundance and categorization of beached litter and on its spatio-temporal variability have been conducted on beaches around the world (e.g., Walker et al., 1997; Williams and Tudor, 2001; Kusui and Noda, 2003; Ivar do Sul and Costa, 2007; Ryan et al., 2009; Ribic et al., 2012). These surveys have generally clarified the present environmental conditions of the beaches and, in some cases, their variability trends. On the other hand, when we assess the impacts of the litter on the beach environment and/or take measures for some scenarios of natural disasters or run-off accidents, it becomes crucial to understand how the beach responds to marine litter inputs from offshore. More specifically, we need to answer the following questions: If a beach receives time-invariant litter input, to what amount does the beached litter finally approach? What is the relaxation time to reach a steady state? And when the litter input varies with time, what are the amplification factor and the phase lag between the input and the abundance on the beach?

Mark-recapture (MR) experiments have been utilized for estimating population and other population parameters such as the survival, recruitment, and population growth rate of animals and fishes (e.g., Peterson and Cederholm, 1984; Smith et al., 1999). The MR method has been applied to beached litter studies by some researchers (e.g., Garrity and Levings, 1993; Bowman et al., 1998; Williams and Tudor, 2001.). In these experiments, all of the target items were sprayed with the same color in accordance with the experimental dates or locations of strandlines where the items were found. This method allows us to understand the population decay and movement of each cohort, but not the movements of individual items.

Garrity and Levings (1993) found that debris tended to move upshore of strandlines and then enter into upland areas, and that the movement of debris was seasonal with greater rates of disappearance out of transects in the dry season than the wet season. They speculated that the average residence time on beaches is less than 1 year. From comparative analyses of the MR experiment results from the six Israeli Mediterranean beaches, Bowman et al. (1998) concluded that beach geomorphology – beach width, ridge and runnel morphology, and beach porosity – made the backshore of beaches an efficient trap for litter. Williams and Tudor (2001) revealed that the residence time of litter on the beach surface

* Corresponding author. Tel.: +81 46 844 5025; fax: +81 46 844 1145.
E-mail addresses: kataoka-t852a@ysk.nilim.go.jp (T. Kataoka), hinata-h92y2@ysk.nilim.go.jp (H. Hinata), s-kato@ace.tut.ac.jp (S. Kato).

0025-326X/$ - see front matter © 2013 Elsevier Ltd. All rights reserved.
http://dx.doi.org/10.1016/j.marpolbul.2013.09.049

depended on its size: items smaller than the substrate size had shorter residence times mainly because they became buried in the beach.

In terms of linear system analysis, the decrease in population of each cohort describes the unit impulse response (UIR) of a beach system. Once we obtain the UIR, we are able to understand the beach response to the time-variant/invariant inputs and thus answer the questions. Here we consider Wadahama Beach as a linear black box and calculate the UIR of target litter items based on MR experiments to acquire an overall understanding of the beach response to marine litter input regardless of seasonality and positions of individual items. We also conducted a dynamic examination of the beach system using a diffusion equation to deduce factors which determine the system characteristics. The target litter items of this study are three types of plastic fishing floats (see Section 2.1), which are comparatively small and hardly moved by wind pressure on the beach. The UIR would depend on litter items, that is, Wadahama Beach would have different system characteristics for other litter items, such as plastic PET bottles, plastic bags and expanded polystyrene floats, whose behavior on the beach is greatly affected by the wind.

2. Materials and methods

2.1. Study site and target items

Wadahama Beach is located on the west coast of Nii-jima Island, about 150 km south of Tokyo (Fig. 1a). There are two isolated mountains in the northern and southern parts of the island. When the Kuroshio Current takes the nearshore nonlarge meander path or the large meander path (e.g., Hinata et al., 2005), the current strikes the west coast of the island. The beach is 900 m long and 30–50 m wide (Fig. 1b), with coarse sand with a mean sediment diameter of $d_{50} = 1.43$ mm. The angle of the beach slope ranges from about 5° to 10°. The coastal hinterland connects the beach with an escarpment with an average angle of about 35° (Fig. 1b). This steep escarpment blocks migration of the beached litter to the hinterland except litter of lower density, such as plastic PET bottles, plastic sheets and plastic bags. The beach is not a public bathing site and thus generally there are few visitors to the beach even in summer. Also, we have not found any people on the beach in the images taken every two hours by the webcam system (Kataoka et al., 2012) which has been installed on the northern hinterland since August 2011 (Fig. 1b).

There are no available measurements of long-term surface wave or sea level data around the island. Instead, we used wind data from the Japan Meteorological Agency (JMA) weather station located in the central region of the island (Fig. 1a). The mountain behind the beach would create local characteristics of the wind field on and around the beach by blocking the easterly winds. Typhoons passing by the island during the summer and autumn seasons will episodically produce larger and longer sea surface waves. We also analyzed the sea level record measured at Oshima Island, which is situated about 50 km north of Nii-jima Island, to understand the Kuroshio Path variability (Fig. 1a).

The target litter items are three types of plastic fishing floats (Fig. 1d). The dimensions and average weights of these floats measured in situ are: type 1: 13.0 cm × ϕ_{max} 2.4 cm, on average 38.8 g; type 2: 13.1 cm × ϕ_{max} 7.8 cm, on average 116.9 g; type 3: 11.0 cm × ϕ_{max} 1.9 cm, on average 12.8 g. We have seen that the floats on the beach are hardly moved even by the strong westerly winter monsoon. We have found all three types of floats stranded on eight beaches distributed from the northernmost to the southernmost ends of the Japanese Archipelago, where we have installed the webcam beached litter monitoring system (Kataoka et al., 2012). Thus, in the future, the system characteristics of Wadahama Beach for the floats revealed in this study will be compared with those of the beaches based on the MR experiments, which will improve our understanding of the beach systems. In addition, Nakashima et al. (2012) found that the type 1 plastic floats contain a high concentration (13.5 ± 8.4 g/kg) of lead (Pb) which could leach into surrounding water in beaches. Thus, it is important to establish a method of calculating the residence time of floats on actual beaches in order to estimate the total mass of Pb leaching into the natural environment.

2.2. Mark-recapture experiments

Mark-recapture experiments have been conducted since September 2011 at one- to three-month intervals (Table 1). The first and second experiments were carried out in the northernmost 100 m- and 200 m-long areas, respectively (Fig. 1b), while the other experiments covered the entire beach. All the target items on the beach were collected, numbered with a permanent marker and replaced where they were found. The number consists of an experiment number and a sequential number allocated to each type of float (Fig. 1d). A thorough search for floats was conducted until no unnumbered target items could be found by repeated observations. The positions of all the items were recorded by a handheld GPS receiver (GARMIN GPSMAP 60CSx) with a measurement error of about ±3 m (Fig. 1b). In addition, the topography of the beach was measured by a real-time kinematic GPS system (Trimble 5800 II, Trimble) with horizontal and vertical measurement errors of about ±5 mm (Fig. 1b). The distance between adjacent measurement points is about 10 m. Based on the experiments, we calculated the numbers of floats that had beached (immigration) and backwashed (emigration) or been buried during the previous and present MR experiments and those of floats that remained on the beach surface. Since we consider the beach as a linear black box, we used the positioning data of individual floats only for setting the initial conditions of the one-dimensional diffusion equation given in Section 4.

2.3. Linear system analysis

Generally, a linear black box is described by a convolution integral. Specifically, in the time-domain, output $y(t)$ is described by the convolution integral of input $x(t)$ and UIR $h(t)$ as follows:

$$y(t) = \int_{-\infty}^{t} x(\tau)h(t-\tau)d\tau. \tag{1}$$

Here in this study, $x(t)$ is the immigration (litter input flux) and $y(t)$ is the total remnant on the beach. $h(t)$ denotes the remnant function of each cohort. From the MR experiments, we calculated $x(t)$, $y(t)$ and $h(t)$.The Fourier transform of Eq. (1) yields

$$Y(\omega) = H(\omega)X(\omega), \tag{2}$$

where $\omega = 2\pi/T$ is the angular frequency and T the period of temporal variability of the input. Eq. (2) describes the system in the frequency domain. $H(\omega)$, the Fourier transform of the UIR, is the frequency response of the system:

$$H(\omega) = \int_{0}^{\infty} h(t)\exp(-i\omega t)dt. \tag{3}$$

The amplitude and the phase response of the system become

$$A(\omega) = |H(\omega)|, \quad \theta(\omega) = \tan^{-1}\frac{\mathrm{Im}(H(\omega))}{\mathrm{Re}(H(\omega))}. \tag{4}$$

Eq. (4) shows that the system characteristics are fully described by the UIR, which can be determined by the MR experiments.

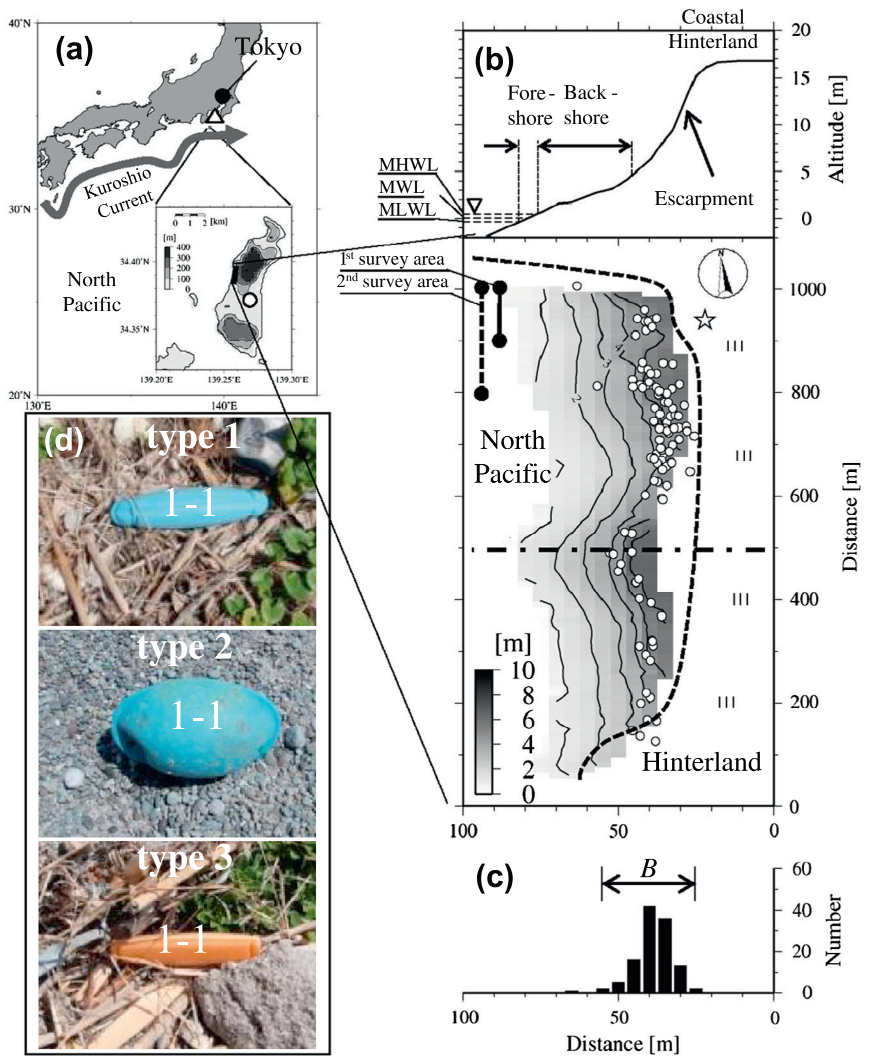

Fig. 1. (a) Location and enlarged map of Nii-jima Island. White triangle indicates the location of the tidal station at Oshima Island of the Japan Meteorological Agency (JMA). In the enlarged map, the altitudes of Nii-jima Island (contour lines and gray-white gradation) and the meteorological observatory of the JMA (white circle) are shown. (b) Enlarged map of Wadahama Beach showing the altitudes (contour lines and gray-white gradation) and positions of target items newly washed ashore from the third to the sixth experiments (white circles), and the position of the webcam (white star). Note that the scale in the latitudinal direction is six times as large as that in the longitudinal direction. The upper panel of (b) shows the cross-sectional beach topography along the dash-dotted line in the lower panel. MHWL, MWL and MLWL represent respectively the mean high water level, the mean water level and the mean low water level calculated from the sea level records obtained during September 2011 to May 2013 at the JMA tide station (see also Fig. 3a). (c) Cross-sectional distribution of the total abundance of immigration from the third to the sixth experiments. B represents the backshore width. (d) Pictures of target items. The numbers on the items, which are used for identifying each item, consist of an experiment number and a sequential number allocated to each type.

Table 1
Cohort population and abundance of re-emergence (within parentheses) in each MR experiment. The abundance of re-emergence is added to the cohort population of the previous experiments. The totals of remnant and re-emergence (within parentheses) in each experiment are shown in the last column.

Experiment number	Experiment date	Cohort no.												Remnant
		1	2	3	4	5	6	7	8	9	10	11	12	
1	2011/09/30	47(0)	–	–	–	–	–	–	–	–	–			47(0)
2	2011/10/27	36 (0)*	76(0)	–	–	–	–	–	–	–	–			112(0)
3	2011/11/24	34(1)	70(0)	62(0)	–	–	–	–	–	–	–			166(1)
4	2011/11/26	34(2)	70(2)	59(0)	20(0)	–	–	–	–	–	–			183(4)
5	2012/01/26	28(2)	51(5)	45(0)	15(0)	18(0)	–	–	–	–	–			157(7)
6	2012/03/23	17(0)	37(2)	35(6)	12(4)	11(0)	18(0)	–	–	–	–			130(12)
7	2012/06/29	12(3)	27(9)	25(7)	6(1)	8(3)	7(0)	136(0)	–	–	–			221 (23)
8	2012/08/21	10(0)	22(1)	21(0)	5(0)	7(0)	6(0)	116(0)	26(0)	–	–			213(1)
9	2012/11/08	6(3)	11(4)	13(2)	4(1)	4(0)	2(0)	48(3)	8(0)	57(0)	–			153(13)
10	2012/12/27	6(0)	9(3)	11(3)	4(3)	4(2)	2(1)	45(2)	8(1)	50(0)	20 (0)			159(15)
11	2013/02/27	6(1)	7(0)	9(0)	3(0)	2(0)	2(0)	37(1)	6(0)	44(4)	16 (0)	28 (0)		160(6)
12	2013/05/08	6(3)	5(0)	6(4)	0(0)	2(1)	0(0)	33(23)	5(3)	29(18)	14(7)	13(0)	191(0)	304(59)

* Population of cohort no. 1 in the second experiment is not used in Figs. 3 and 4 because the second experiment was carried out in the northernmost 200 m-long area.

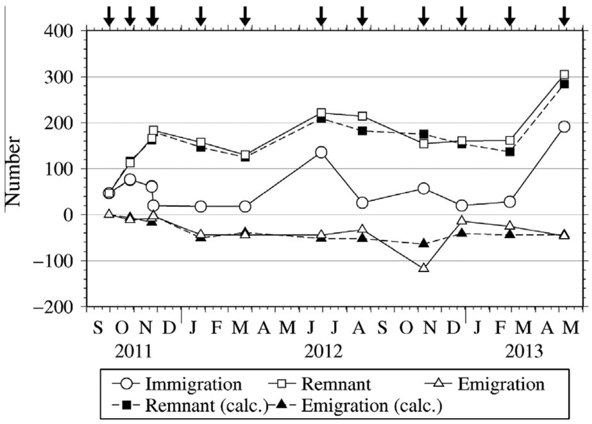

Fig. 2. Time series of the total numbers of immigration, remnant and emigration revealed by the MR experiments. Dashed lines with solid symbols show the time series of the remnant and the emigration calculated from the observed immigration using Eqs. (1) and (5). Black arrows show the date of each experiment.

3. Results

3.1. System characteristics of Wadahama Beach

The time series of the total immigration ($x(t)$), remnant ($y(t)$) and emigration ($z(t)$) of all types are shown in Fig. 2. The total immigration has local maximums in October 2011 and June 2012, whereas the total emigration takes local maximums in January and November 2012. The resultant total remnant has local maximums (minimums) in November 2011 and June 2012 (in March and November 2012).

Generally, the time series ($x(t)$, $y(t)$, $z(t)$) of each float type (not shown here) has local maximums and minimums in the corresponding months of the time series of the totals shown in Fig. 2. The similar temporal variation pattern of immigration suggests that all types have similar spatial distribution and drifting characteristics in the offshore, while the similar emigration time series would be the result of similar movements of all the types on the beach. Thus, here we derived the UIR regardless of the float type.

The population decay of each cohort is tabulated in Table 1. The remnants include the number of re-emerged floats which were not recovered in the previous surveys but were found in the present survey. However, the ratio of re-emerged floats to the remnants is very small (6% on average). Natural or anthropogenic large debris, such as logs and lumbers, was not common on the beach: it did not form any strandline, but was stranded separately and sparsely. In the experiments, we searched for the target items behind and beneath such debris. Presumably, re-emerged floats had been buried in the sand. Williams and Tudor (2001) found that litter items larger than the surrounding substrate accumulated more readily on the beach surface, since these items would be exhumed by energetic wind waves. Thus, we assume that the emigration of the floats is mainly driven by backwashing to the sea.

Fig. 3 shows the time series of the 30-day moving averages of adjusted sea level (Fig. 3a), monthly wind velocity and direction (Fig. 3b), and the population decay of all the cohorts normalized by the initial input values (Fig. 3c). The positive sea level anomaly corresponds well with the Kuroshio Path variation: the Kuroshio took the nearshore nonlarge meander path and would hit Nii-jima Island in September 2011, May 2012, from September to November 2012 and in April 2013 (http://www1.kaiho.mlit.go.jp/KANKYO/KAIYO/qboc/index_E.html). Although the sea level changes due to tide (by about ±40 cm) around Nii-jima Island, we are unable to discuss the relation between the population decay revealed by bimonthly MR experiments and tide-induced sea level changes. For the wind fields, weaker easterly winds dominated in summer whereas stronger westerly winds prevailed from late autumn to early spring.

In general, the populations decrease exponentially with lower (higher) decreasing rates from June to August 2012 and from

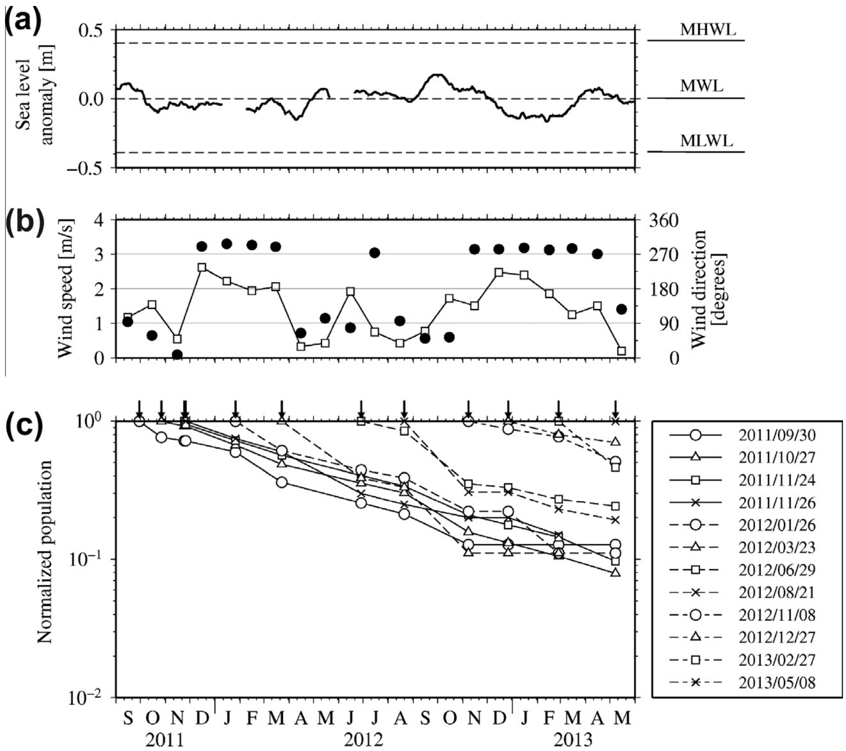

Fig. 3. Time series of (a) 30-day moving average of adjusted sea level anomaly at the JMA tidal station (see white triangle in Fig. 1a), (b) monthly average wind speed (solid line with white square) and direction in degrees clockwise from north (black circle) observed at the JMA wind station (white circle in Fig. 1a) and (c) the population decay of each cohort. Black arrows in (c) show the date of each experiment.

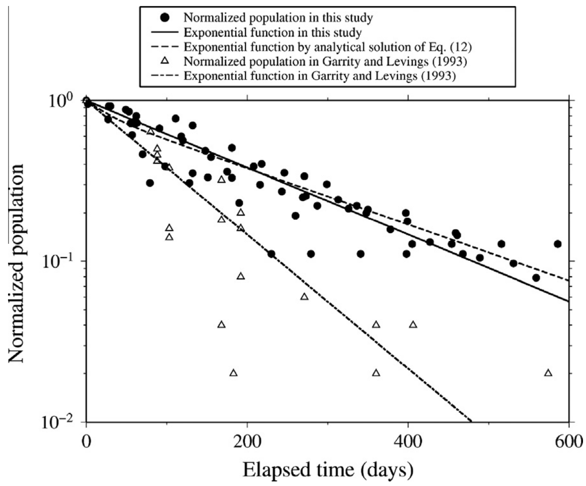

Fig. 4. Unit impulse response functions revealed by all the MR experiments of Wadahama Beach (solid line) and from the MR experiments by Garrity and Levings (1993) (dash-dotted line) which was calculated by reading the value of the cohort population from their Fig. 3. The dashed line represents the normalized population decay obtained by solving the diffusion Eq. (12) with the diffusion coefficient set to 0.17 $cm^2 s^{-1}$.

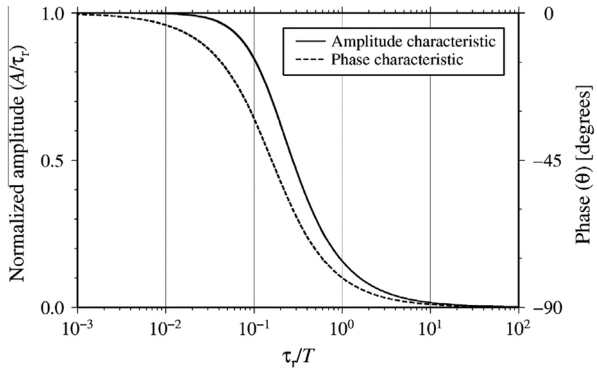

Fig. 5. System characteristics of Wadahama Beach as functions of τ_r/T.

November 2012 to March 2013 (August to November 2012). There was no significant relationship between the temporal variability of sea level record and that of the decreasing rates. On the other hand, local maximums of the immigration in June 2012 and May 2013 (see Fig. 2) were preceded by the nearshore nonlarge meander path, which suggests that the Kuroshio plays an important role in the transportation of the target items. Unexpectedly, a significant relationship was not found between the temporal change in the rates and that in the monthly wind velocity. In actuality, the floats on the beach may be backwashed intermittently to the sea by storm events which are not represented by the monthly average wind velocities; however, we will not examine here the mechanisms of the temporal change in the decreasing rates.

The plot of the normalized population made from all the experiment data setting the experiment dates equal to 0 (Fig. 4) provides a much clearer exponential decay. We approximated the plots as an exponential function ($\exp[-kt]$) with 95% confidence level ($R^2 = 0.867$, $P < 0.01$) and obtained the UIR function of the beach for the target items as follows:

$$h(t) = \begin{cases} \exp(-\frac{t}{209}), & (t \geq 0), \\ 0, & (t < 0), \end{cases} \tag{5}$$

where t is elapsed time in days. From the integral of this function from $t = 0$ to infinity, the residence time of the floats on the beach is estimated as $\tau_r = 1/k = 209$ days, that is, about seven months. From Eqs. (3)–(5), we obtain the Wadahama Beach system characteristics as functions of τ_r/T (Fig. 5):

$$A\left(\frac{\tau_r}{T}\right) = \frac{\tau_r}{\sqrt{1 + (2\pi\frac{\tau_r}{T})^2}}, \theta\left(\frac{\tau_r}{T}\right) = -\tan^{-1}\left(2\pi\frac{\tau_r}{T}\right). \tag{6}$$

The amplification factor A/τ_r and the phase lag (not time lag) respectively approach 1 and 0 as $\tau_r/T \to 0$. For $\tau_r/T \gg 1$, $A/\tau_r \approx 0$ and $\theta \approx \pi/2$. Practically, time-variant float inputs with a much shorter period than the residence time, such as $T < 20$ days ($\tau_r/T > 10$), would have almost no impact on the beach environment.

We calculated the remnants ($y(t_i)$) from the observed immigrations ($x(t_1), x(t_2),\ldots,x(t_i)$) by using Eqs. (1) and (5), where t_i is the date of the i-th experiment. Then the emigrations were calculated as $z(t_i) = (y(t_i) - y(t_{i-1})) - x(t_i)$. Fig. 2 shows that the calculated remnants and emigrations agree well with the corresponding observation results except in November 2012. Although the discrepancy appears to arise from the exclusion of the temporal change in the decreasing rate, this overall agreement confirms that the beach responds linearly to the float inputs. At present it is difficult to perform precise frequency analyses on the time series of the immigrations and remnants and on their relations based on twelve MR experiments. In the future, much longer MR experiments or experiments with shorter time intervals will allow us to conduct, for instance, Fourier transformation and correlation analysis of the time series.

Despite the inclusion of the data from the first and second experiments in which the survey areas were limited to the northern part of the beach, the calculated remnants and emigrations correspond well with the observed ones (Fig. 2). The temporal decay of the first and second cohorts' population indicates the residence time of the floats, which had washed ashore in the northern part of the beach, on the whole Wadahama Beach. From the third to the sixth experiment, 19 (50)% of the immigrations were found within the northernmost 100 (200) m-long area. Thus, the decay exhibited by the first and second experiments would describe the overall system characteristics of the whole beach.

3.2. Beach response to idealized inputs

To answer the question raised in Section 1, here we calculate the beach response to idealized inputs. The time evolution of the abundance of the remnants on the beach is calculated by Eq. (1), whereas Eq. (6) gives the beach response in the steady-state. First, assuming that Wadahama Beach receives a time-invariant litter input flux of x_0 (ind./day) after a total clearance of beach litter, that is, $y(0) = 0$, the time evolution becomes

$$y(t) = \int_0^t x_0 \exp\left(-\frac{t-\tau}{\tau_r}\right) d\tau = \tau_r x_0 \left[1 - \exp\left(-\frac{t}{\tau_r}\right)\right]. \tag{7}$$

The second term of the right-hand side is a decay term. The abundance finally approaches $y_\infty = \tau_r x_0 = 209 x_0$ as $t \to \infty$. The abundance reaches 90% of y_∞ at $t_{90} = -\tau_r \times \ln(0.1) = 2.3\tau_r = 481$ - days. The relaxation time t_{90} is proportional to the residence time of the beach, not depending on the litter input flux. If a beach that has an exponential decay type of the UIR and much longer residence time receives the constant litter input of x_0, the litter slowly but greatly accumulates on the beach.

Second, the beach response to a sinusoidal input with an amplitude of x_0 (ind./day) and with a period of T_0 (day) is calculated. Although a negative litter input is not realistic, this does not cause any problem when analyzing the basic characteristics of the beach system. The response becomes

$$\begin{aligned} y(t) &= \int_0^t x_0 \sin\left(\frac{2\pi}{T_0} t\right) \exp\left(-\frac{t-\tau}{\tau_r}\right) d\tau \\ &= A x_0 \left[\sin\left(\frac{2\pi}{T_0} t + \theta\right) - \sin\theta \cdot \exp\left(-\frac{t}{\tau_r}\right)\right], \end{aligned} \tag{8}$$

where A and θ are the amplification factor and phase lag in Eq. (6), respectively. Generally, the decay term in Eq. (8) is much smaller than that in Eq. (7). If the input varies seasonally with a period of one year, the maximum of the remnants on the beach appears at about 75 days after the input maximum. If the beach receives a combined input, which is a more realistic input, the abundance approaches.

$$y(t) \to x_0 \left\{ \tau_r + A \sin\left[\frac{2\pi}{T_0} t + \theta\right] \right\}, (t \to \infty), \tag{9}$$

as predicted by Eq. (6). In this case, the relaxation time is almost determined by the decay term for the constant input. Specific examples of the response of Wadahama Beach with $x_0 = 1$(ind./day) and T_0 (=$2\pi/\omega_0$) = 180 days are shown in Fig. 6.

If the inputs of the floats ($x(t)$) to Wadahama Beach are given according to some scenarios based on numerical models (e.g., Kubota, 1994; Kako et al., 2011; Potemra, 2012; Maximenko et al., 2012), we can estimate the time evolution of the abundance on Wadahama Beach ($y(t)$). Conversely, when $y(t)$ is measured by the webcam system or beach surveys by humans, $x(t)$ can be estimated by the inverse Fourier transform of $X(\omega) = Y(\omega)/H(\omega)$ and then compared with the model predictions, which is useful for improving the numerical models. We note that existing numerical models calculate the abundance of litter on the sea surface but not on beaches, and that the linear system analysis serves as a mediator between numerical models and beach monitoring.

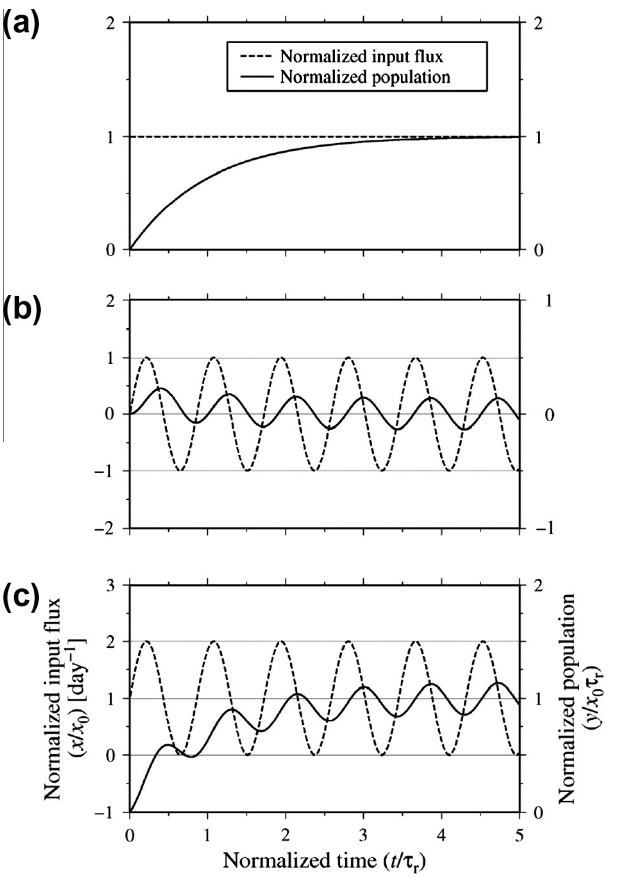

Fig. 6. The response of Wadahama Beach to idealized inputs. The responses to constant litter input flux (a), sinusoidal litter input flux (b) and combined litter input flux (c), respectively. The legends of the lines are shown in (a).

4. Discussion

Naturally, the following two questions arise from the above linear system analysis: What are the factors determining τ_r? Do all beaches have an exponential decay type of unit impulse response? If a beach has an exponential decay type of unit impulse response ($\exp[-t/\tau_r]$), the system characteristics of the beach are fully determined by τ_r. However, it is not realistic to conduct long-term MR experiments of all beaches involving human effort. If we can understand the factors and develop a mathematical model of τ_r, for instance, as a function of hydro- and morphodynamic statistics, we will be able to produce a residence time map for a region of interest with much less effort. The map would allow us to assess the long-term impacts of marine litter caused by natural disasters and/or loss of flow accidents on beaches and to take measures to minimize the overall damage in the region.

4.1. Governing equation of population decay

Before discussing the questions, dynamic investigations of the system will be helpful. From Eq. (5), the population of each cohort obeys the following equation:

$$\frac{dy_c(t)}{dt} + \frac{y_c(t)}{\tau_r} = 0 \tag{10}$$

The outflow flux from the beach to the sea is proportional to the population itself. The solution of Eq. (10) becomes

$$y_c(t) = y_c(0) \exp\left(-\frac{t}{\tau_r}\right) = y_c(0)\gamma^t, \tag{11}$$

where $\gamma = \exp[-1/\tau_r]$ is the mean unit-time survival rate on the beach. This solution denotes that randomly selected floats of $y_c(1-\gamma)$ backwash to the sea in every unit time. The residence time of 209 days of the floats on Wadahama Beach corresponds to a daily survival rate of 99.5%, that is, a yearly survival rate of 17.4%. This implies that the backwash process can be described by a random diffusion process, in which case the governing equation is considered to be:

$$\frac{\partial \rho(x,t)}{\partial t} = D \frac{\partial^2 \rho(x,t)}{\partial x^2} \tag{12}$$

where the x-axis points positive in the offshore direction with the origin at the landward edge of the backshore (see Fig. 7), D is a time-invariant diffusion coefficient and $\rho(x, t)$ is the number of floats per unit length. Since we have not found any floats on the hinterland or foreshore of the beach, the boundary conditions are

$$\begin{cases} D\frac{\partial \rho}{\partial x} = 0, & (x = 0), \\ \rho = 0, & (x \geqslant B), \end{cases}$$

where B denotes the backshore width. Integrating Eq. (12) from $x = 0$ to $x = B$ with a boundary condition of no net flux at $x = 0$ gives

$$\frac{dy_c(t)}{dt} = D \left.\frac{\partial \rho}{\partial x}\right|_B. \tag{14}$$

The order of D can be estimated by comparing Eq. (14) with Eq. (10):

$$-\frac{y_c}{\tau_r} = D \left.\frac{\partial \rho}{\partial x}\right|_L \approx D \frac{-y_c/B}{B} = -D\frac{y_c}{B^2}.$$

$$\therefore D \approx \frac{B^2}{\tau_r}. \tag{15}$$

Substituting $B = 30$ m and $\tau_r = 209$ days into Eq. (15), D is of the order of $10^{-1}\,\mathrm{cm^2\,s^{-1}}$. The solution of Eq. (12) subject to the boundary conditions of Eq. (13) is

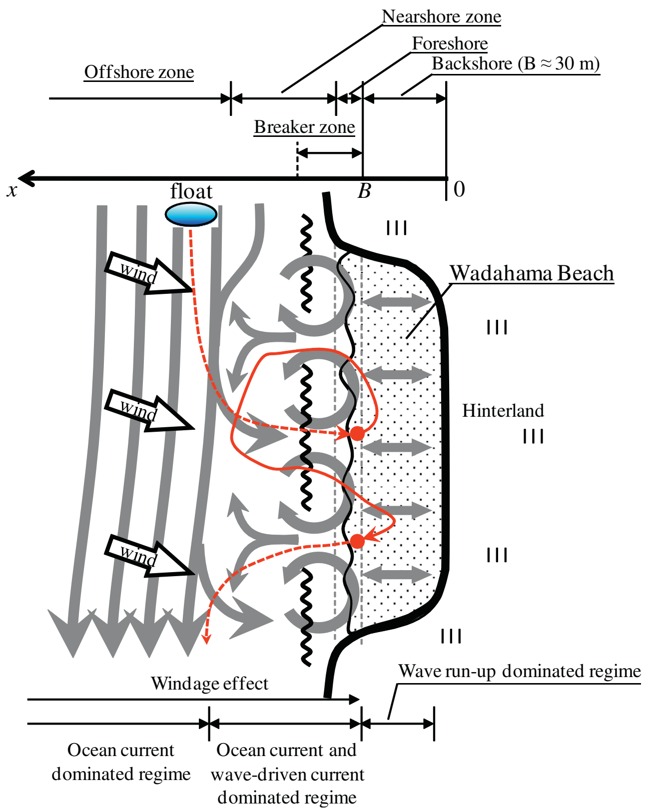

Fig. 7. Schematic image of current regimes and the behavior of a target float (red lines) on and around Wadahama Beach with the coordinate used for one-dimensional diffusion calculation. B represents the location of the boundary between the foreshore and backshore. Residence time (τ_r) corresponds to the time taken for the float to move along the bold red line. However, the time taken for drifting in the nearshore region is considered to be much shorter than the duration for which the float stays on the beach. (For interpretation of the references to colour in this figure legend, the reader is referred to the web version of this article.)

$$\begin{cases} \rho(x,t) = \sum_{n=1}^{N} \alpha_n \exp(-\lambda_n^2 Dt)\cos(\lambda_n x), \\ \alpha_n = \frac{4\lambda_n}{\sin(2\lambda_n B)+2\lambda_n B}\int_0^B \rho(x,0)\cos(\lambda_n x)dx, \end{cases} \quad (16)$$

where λ_n (=(2n-1)π/2B) is the eigenvalue of the n-th mode and N the highest mode number. The population of the cohort is then obtained by integrating the density over the backshore width:

$$y_c(t) = \int_0^B \rho(x,t)dx. \quad (17)$$

From the individual float positioning survey results (Fig. 1c), we assumed a sinusoidal initial distribution of the floats as follows:

$$\rho(x,0) = \begin{cases} \frac{\pi}{2B}\sin(\frac{\pi x}{B}), & (0 \leqslant x < B), \\ 0, & (x < 0,\, x \geqslant B). \end{cases} \quad (18)$$

The population decay obtained by substituting Eqs. (16) (N = 10) and (18) into Eq. (17) and setting D equal to 0.17 cm^2 s^{-1} reproduce well the UIR function from the MR experiments (Fig. 4). Although the value of D was actually adjusted so that the population decay agrees well with the UIR from the MR experiments, it is important to note that the order of D is in accordance with Eq. (15). This demonstrates that the long-term float population dynamics on Wadahama Beach are governed by a diffusion equation and that the order of the diffusion coefficient can be estimated from the residence time and the backshore width.

4.2. Factors determining τ_r

From the individual float positions recorded by the handheld GPS receiver, it was found that the population of each cohort decreased exponentially as the floats changed position laterally and longitudinally (not shown here). Considering that the wind has little effect on the movement of floats on the beach, this implies that the exponential decay results from iteration of the following sequential dynamic processes: washing ashore the beach – backwashing to the sea – drifting in the nearshore region – washing ashore again/drifting far offshore (Fig. 7). The drifting of the floats on the sea surface is affected by the wind. Therefore, the resultant residence time τ_r will depend on the statistics of wind-waves, wind- and/or wind-wave-driven coastal currents and winds in the nearshore region.

Eq. (15) shows that the determination of τ_r can be replaced by a derivation of the diffusion coefficient D, which more directly explains the hydrodynamics. Let us consider two beaches with widths of B and $2B$, having the same residence time of τ_r. The diffusion coefficient of the wider beach is about four times as large as that of the narrower beach, which would be the result of more energetic wave-current systems. Conversely, when the two beaches have the same hydrodynamic statistics, Eq. (15) suggests that the wider beach would have even longer residence time, that is, a much higher abundance of litter.

From comparisons of the MR experiment results on six Israeli Mediterranean beaches, Bowman et al. (1998) concluded that swash energy to beach width and beach morphology are the dominant factors controlling the quantity of litter on the beaches. They found that the two widest beaches had the most litter. Tsouk et al. (1985) reached the same conclusion in their study on oil-polluted Israeli beaches. Their widest beach ranked lowest in self-cleaning performance. Bowman et al. (1998) also reported that high beach porosity is the most dominant physical factor, because it increases the subsurface beach drainage and diminishes the backwash of litter, thus preventing self-cleaning and encouraging litter accumulation. Williams and Tudor (2001) revealed that the residence time of litter on the beach surface depended on litter size: items that were smaller than the substrate had a shorter residence time mainly due to burial of items in the beach.

When we consider the residence time of litter with lower densities such as PET bottles and plastic bags, wind pressure force acting on the beached litter surface seems to be a crucial factor, since we frequently found that, for instance, plastic bags were moved down to the foreshore or up to the escarpment from the backshore of the beach by wind pressure, which appears to reduce the residence time of such litter on the beach.

From the above discussions, generally, τ_r of litter on a beach is considered to be given by

$$\tau_r \approx \frac{B^2}{D(S,\, W,\, d_{50},\, \rho_l,\, l)}, \quad (19)$$

where S is wave-current field statistics, W the statistics of wind field, d_{50} the mean sediment diameter, ρ_l the density of the litter and l the representative length of the litter. The density is included to represent litter behavior on a beach and in its offshore. For the target floats, the wind statistics affect τ_r via the wave-current fields and wind effects in the nearshore.

4.3. The UIR function of the beaches on the Caribbean Coast

Garrity and Levings (1993) identified the temporal decay of fifty representative items in a 1 × 50 m transect at four sites along the Caribbean Coast of Panama. In general, the number of each item in the four transects exponentially decreased with respect to time, as shown in their Fig. 3. They did not show specific data on the population decay. Thus, by reading the population decays from the figure and combining all the data from the four sites, we approximated the time decay as an exponential function ($\exp[-kt]$) with 95% confidence level ($R^2 = 0.769$, $P < 0.01$) as follows (dash-dotted line in Fig. 4):

$$h(t) = \begin{cases} \exp\left(-\frac{t}{104}\right), & (t \geqslant 0), \\ 0, & (t < 0). \end{cases} \tag{20}$$

From this equation, the residence time is found to be 104 days, which is half the residence time of Wadahama Beach probably due to the following two reasons: (1) The transect area (1×50 m) is much smaller than that of Wadahama Beach ($30–50 \times 900$ m); and (2) the representative items included litter with lower density such as Styrofoam, which was the second most abundant categories on the transect and is likely to be moved by wind.

This suggests that other beach systems could have exponential decay type of UIR, and also that the residence time depends on the dimensions of the particular site and the litter items. This finding supports the above discussion on the residence time and diffusion coefficient based on our MR experiments.

5. Conclusion

The exponential decay of the amount of new fishing floats on Wadahama Beach, Nii-jima Island, Japan revealed by 20-month mark-recapture (MR) experiments demonstrated a linear response of the beach to the input of litter. By approximating the decay as an exponential function, we obtained the unit impulse response (UIR) of the linear beach system. Also, we obtained the system characteristics from the Fourier transform of the UIR.

The characteristics are fully determined by the residence time (τ_r) of the floats on the beach and can be described as functions of the ratio of τ_r to periods of the float input variability (T). The amplification factor A/τ_r and the phase lag (not time lag) respectively approach 1 and 0 as $\tau_r/T \to 0$. For $\tau_r/T \gg 1$, $A/\tau_r \approx 0$ and $\theta \approx \pi/2$. Practically, time-variant float inputs with a much shorter period than the residence time would have almost no impact on the beach environment.

Assuming idealized time-invariant and/or variant litter input fluxes, time evolutions of the abundance on Wadahama Beach were examined by using the convolution integral of the inputs and the UIR. When the beach receives the combined litter flux, the abundance reaches a dynamic steady-state in about twice the residence time, where the relaxation time is determined by the time-invariant component of the input.

Combinations of existing ocean models and linear system analysis would allow us to predict the abundance of litter on beaches by the convolution integral of the model-derived input and the UIR of the beaches. Conversely, it is possible to estimate the inputs from the abundance of litter on beaches measured by webcam systems or human beach surveys, then the calculated inputs could be compared with the results of existing ocean models and used to improve the models.

The exponential decay was well reproduced by a diffusion equation with a constant diffusion coefficient, whose order of magnitude was found to be roughly estimated by the backshore width and the residence time of the floats. This demonstrates that determination of τ_r can be replaced by a derivation of the diffusion coefficient, which more directly explains the hydrodynamics. From our MR and individual float positioning experiments as well as the results of previous studies, the coefficient would depend on wave-current and wind-field statistics and beach geomorphology as well as the density of the litter.

This study identified the characteristics of the Wadahama Beach system for three types of floats. To understand more comprehensively the mechanisms that determine τ_r or its equivalent, the diffusion coefficient, long-term MR and individual float positioning experiments are required for various debris items on different beaches which have different specific morphologies and wave-current and wind-field statistics.

Acknowledgements

We sincerely thank Dr. Atsuhiko Isobe of Ehime University, Dr. Masahisa Kubota of Tokai University, Dr. Hideshige Takada of Tokyo University of Agriculture and Technology, Dr. Shin'ichi Aoki of Osaka University and Drs. Takanobu Inoue and Takumi Okabe of Toyohashi University of Technology for their valuable comments. The authors also sincerely thank Mr. Ryotaro Fuji of Kokusai Kogyo Co., Ltd. for assistance with the MR experiments. This research was supported by the Environment Research and Technology Development Fund (B-1007) of the Ministry of the Environment, Japan and by JSPS KAKENHI Grant Numbers 23656309, 25820234.

References

Bowman, D., Manor-Samsonov, N., Golik, A., 1998. Dynamics of litter pollution on Israeli Mediterranean beaches: a budgetary, litter flux approach. Journal of Coastal Research 14 (2), 418–432.

Garrity, S.D., Levings, S.C., 1993. Marine debris along the Caribbean Coast of Panama. Marine Pollution Bulletin 26 (6), 317–324.

Hinata, H., Yanagi, T., Takao, T., Kawamura, H., 2005. Wind-induced Kuroshio warm water intrusion into Sagami Bay. Journal of Geophysical Research 110 (C3), C03023.

Ivar do Sul, J.A., Costa, M.F., 2007. Marine debris review for Latin America and the Wider Caribbean Region: from the 1970s until now, and where do we go from here. Marine Pollution Bulletin 54 (8), 1087–1104.

Japan Coast Guard. 2013. Quick Bulletin of Ocean Conditions. WWW page, <http://www1.kaiho.mlit.go.jp/KANKYO/KAIYO/qboc/index_E.html>.

Kako, S.I., Isobe, A., Magome, S., Hinata, H., Seino, S., Kojima, A., 2011. Establishment of numerical beach-litter hindcast/forecast models: an application to Goto Islands, Japan. Marine Pollution Bulletin 62 (2), 293–302.

Kataoka, T., Hinata, H., Kako, S.I., 2012. A new technique for detecting colored macroplastic debris on beaches using webcam images and CIELUV. Marine Pollution Bulletin 64 (9), 1829–1836.

Kubota, M., 1994. A mechanism for the accumulation of floating marine debris north of Hawaii. Journal of Physical Oceanography 24 (5), 1059–1064.

Kusui, T., Noda, M., 2003. International survey on the distribution of stranded and buried litter on beaches along the Sea of Japan. Marine Pollution Bulletin 47 (1), 175–179.

Maximenko, N., Hafner, J., Niiler, P., 2012. Pathways of marine debris derived from trajectories of Lagrangian drifters. Marine Pollution Bulletin 65 (1), 51–62.

Nakashima, E., Isobe, A., Kako, S.I., Itai, T., Takahashi, S., 2012. Quantification of toxic metals derived from macroplastic litter on Ookushi Beach, Japan. Environmental Science & Technology 46 (18), 10099–10105.

Peterson, N.P., Cederholm, C.J., 1984. A comparison of the removal and mark-recapture methods of population estimation for juvenile coho salmon in a small stream. North American Journal of Fisheries Management 4 (1), 99–102.

Potemra, J.T., 2012. Numerical modeling with application to tracking marine debris. Marine Pollution Bulletin 65 (1), 42–50.

Ribic, C.A., Sheavly, S.B., Rugg, D.J., Erdmann, E.S., 2012. Trends in marine debris along the US Pacific Coast and Hawai'i 1998–2007. Marine Pollution Bulletin 64 (5), 994–1004.

Ryan, P.G., Moore, C.J., van Franeker, J.A., Moloney, C.L., 2009. Monitoring the abundance of plastic debris in the marine environment. Philosophical Transactions of the Royal Society B: Biological Sciences 364 (1526), 1999–2012.

Smith, T.D. et al., 1999. An ocean-basin-wide mark-recapture study of the North Atlantic humpback whale (Megaptera novaeangliae). Marine Mammal Science 15 (1), 1–32.

Tsouk, E., Amir, S., Goldsmith, V., 1985. Natural self-cleaning of oil-polluted beaches by waves. Marine Pollution Bulletin 16 (1), 11–19.

Walker, T.R., Reid, K., Arnould, J.P.Y., Croxall, J.P., 1997. Marine debris surveys at Bird Island, South Georgia 1990–1995. Marine Pollution Bulletin 34 (1), 61–65.

Williams, A.T., Tudor, D.T., 2001. Litter burial and exhumation: spatial and temporal distribution on a cobble pocket beach. Marine Pollution Bulletin 42 (11), 1031–1039.